marine drugs

MDPI

Article

Diverse Bioactive Secondary Metabolites from *Aspergillus terreus*: Antimicrobial, Anticancer and Anti- SARS-CoV-2 Activity Studies

Abdelaaty Hamed [1,2], Ahmed S. Abdel-Razek [2♥], Ahmed B. Abdelwahab [3], Ahmed El Taweel [4], Mohamed GabAllah [4], Norbert Sewald [2,*] and Mohamed Shaaban [2,5,*]

[1] Chemistry Department, Faculty of Science, Al-Azhar University, Nasr City-Cairo 11884, Egypt; abdelaaty-hamed.1@azhar.edu.eg.
[2] Organic and Bioorganic Chemistry, Faculty of Chemistry, Bielefeld University, D-33501 Bielefeld, Germany; ahmedshukri_sci@yahoo.com (ASA), norbert.sewald@uni-bielefeld.de (NS).
[3] Lorraine University, L2CM, 1 Boulevard Arago, 57070, France; ahmedbakr81@yahoo.com.
[4] Center of Scientific Excellence for Influenza Virus, Environmental Research Division, National Research Centre,Giza 12622, Egypt; ahmednageh_nrc2009@yahoo.com (AET), gaballah09@gmail.com (MG).
[5] Chemistry of Natural Compounds Department, Pharmaceutical and Drug Industries Research Institute, National Research Centre, El-Buhouth St. 33, Dokki-Cairo 12622, Egypt; mshaaba@gmail.com.
* Correspondence: norbert.sewald@uni-bielefeld.de (NS); mshaaba@gmail.com (MS)
♥ Dedication for our colleague Assoc. Prof. Ahmed S. Abdel-Razek who passed away on 15th November 2021

Abstract: The recently reported microbial natural product N-benzoyl-tryptophane (**1**) along with twenty-two diverse known bioactive compounds were isolated from the marine *Aspergillus terreus* LGO13 after its re-cultivation using liquid culture fermentation. Structures of the isolated compounds were established on the basis of HR-ESIMS 1D/2D NMR spectroscopy, and comparison with literature data. The antimicrobial, cytotoxicity, and antiviral activities of the microbial extract and the obtained compounds were investigated using a set of microorganisms, cervix carcinoma KB-3-1, non-small cell lung cancer (NSCLC) A549, and coronavirus (SARS-CoV-2), respectively. Molecular docking (MD) simulation was employed to explore the theoretical targets of the isolated metabolites as anti-SARS-CoV-2 agents. Chaetominine (**2**) seemed to be a potential candidate against papain-like protease (PLpro), one of the viral proteins being aimed by recent research as a possible target of anti-covid agents. Inspired by the MD results, we accordingly assessed the antiviral efficacy of chaetominine (**2**), fumitremorgin C (**6**), and azaspirofuran A (**9**) against SARS-CoV-2. Fumitremorgin C (**6**) showed a high selectivity index (SI = 20.3), while chaetominine (**2**) and azaspirofuran A (**9**) showed moderate selectivity index (SI = 6.6 and 3.2, respectively). These results showed a promising antiviral activity of Fumitremorgin C against SARS-CoV-2 virus.

Keywords: Marine *Aspergillus terreus*; Bioactive Metabolites; Antimicrobial; cytotoxicity; Anti-coronavirus Activities

Citation: To be added by editorial staff during production.

Academic Editor: Firstname Lastname

Received: date
Revised: date
Accepted: date
Published: date

1. Introduction

Microorganisms isolated from different habitats represent prolific resources of novel and bioactive metabolites which are considered as indication for drug-discovery [1-3]. Fungi have been recently considered a promising source of secondary metabolites that elicited a wide range of beneficial values both on the therapeutic and commercial scales. Recently, fungal metabolites have gained great attention as an everlasting source of precious compounds that can serve as novel entities for various therapeutic approaches [4].

Also, marine-derived fungi have gained significant attention as promising therapeutic approaches for the treatment of a wide array of human ailments and as successful tools for drug discovery [5,6]. This is mainly attributed to their richness by a diverse array of

secondary metabolites. These promising activities are represented by antiviral, antibacterial, anti-inflammatory, and anticancer activity [7].

Aspergillus represents a widely spread genus of fungi that are highly popular for possessing a potent medicinal potential comprising mainly antimicrobial, cytotoxic, and antioxidant activities that are highly attributed to its richness by a wide range of structurally heterogeneous secondary metabolites, namely alkaloids, terpenes, steroids, and polyketides, peptides, and lactones, that are of considerable interest to the scientific research community. Fungi of this genus produce important secondary metabolites that have industrial importance [8,9] and therapeutic significance like antibiotics [10] and lovastatins [11], reflecting the considerable importance of Aspergillus spp. both in the scientific and pharmaceutical industries levels [4,12,13].

Among the Aspergillus spp, *Aspergillus terreus* is well known for its potential as a prolific and great resource of promising and unusual bioactive metabolites [14-17]. Therefore, and during our continual search for diverse bioactive compounds [16] having anti-SARS-CoV-2 activity, a re-cultivation of the marine Aspergillus terreus LGO13 on M2 liquid medium and applying to shaker fermentation followed by working up and chromatographic purification afforded twenty-three diverse bioactive compounds (**1**-**23**) (Fig. 1). The antimicrobial, cytotoxicity and antiviral activities of the microbial extract and obtained compounds were visualized using a set of microorganisms, cervix carcinoma KB-3-1, non-small cell lung cancer (NSCLC) A549, and coronavirus (SARS-CoV-2), respectively. Isolation and taxonomical characterization of the producing microorganism was revealed as well. 3C-like protease (3CLpro), papain-like protease (PLpro), and spike protein S were the biological targets of choice for anti-covid characteristics. These targets have been approached to halt the virus propagation inside the host cells [18].

Coronaviruses are enveloped, positive-sense, single-stranded RNA viruses that are widely dispersed among humans, other mammals, and birds. The cause of respiratory, gastrointestinal, hepatic, and neurological illnesses [19]. In late December 2019, the WHO Office in China was informed of pneumonia cases of unidentified etiology in Wuhan City which were subsequently declared to be associated with a new coronavirus, later known as Severe Acute Respiratory Syndrome Coronavirus 2 (SARS-CoV-2). The devastating expansion of SARS-CoV-2 was faster than any other zoonotic coronavirus [20]. This urged the need to find medications to reduce mortality and the unaffordable hospitalization rates, especially in the absence of effective prepandemic vaccines or antiviral therapeutics. Several trials were performed to re-purpose drugs as a faster way to discover effective drugs in COVID-19 treatment and other natural compounds or metabolites [21,22]. Herein we assess the efficacy of selected metabolites isolated from the marine *Aspergillus terreus* LGO13 based on molecular docking (MD) simulation as antiviral agents against SARS-CoV-2, which focuses on creating innovative antiviral and anticancer drugs while paying close attention to their safety profile for normal cells.

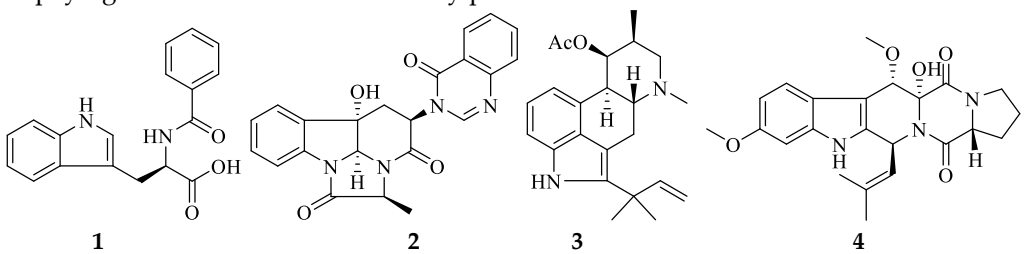

1 **2** **3** **4**

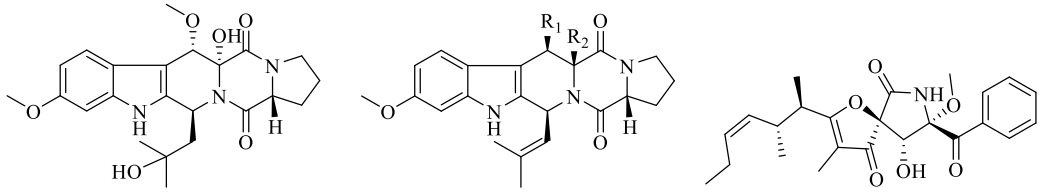

5 **6:** R_1= R_2=H, **7:** R_1=R_2=OH **8**

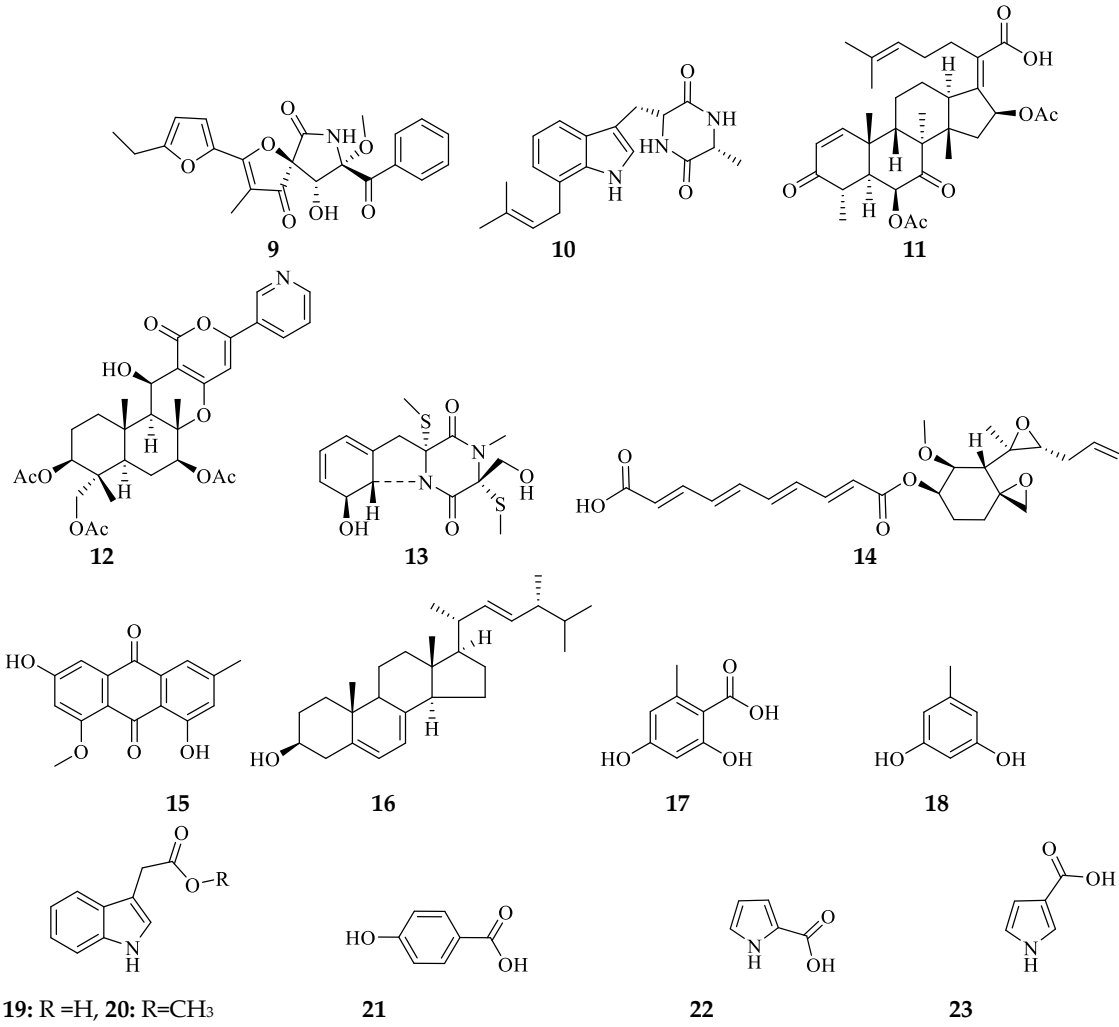

Figure 1. Chemical structures of compounds **1-23**.

2. Results and discussion

2.1. Isolation and Taxonomic Identification of the Producing Fungus

Details of isolation and taxonomic characterization of the extremophilic fungus *Aspergillus terreus* LGO13 were reported recently by our research team [16]. Phylogenetic analyses of the aligned segment of 18S rRNA gene revealed close similarity (99%) of LGO13 to *Aspergillus terreus* [16]. The sequence of the strain has been recorded in GenBank database (accession no. MH470250). The strain LGO13 was cultivated on potato-dextrose agar and kept into refrigerator at 4°C.

2.2. Isolation and structure identification of the Produced Compounds

An application of the marine fungus LGO13 crude extract to a series of diverse chromatographic techniques afforded twenty-three diverse bioactive compounds, namely, the recently reported *N*-benzoyltryptophane (**1**) [23] together with chaetominine (**2**) [24], fumigaclavine C (**3**) [1], cyclotryprostatin B (**4**) [25], 20-hydroxycyclotryprostatin B (**5**) [26], fumitremorgin C (**6**) [27], 12,13-dihydroxyfumitremorgin C (**7**) [28], pseurotin A (**8**) [29], azaspirofuran A (**9**) [30], terezine D (**10**) [31], helvolic acid (**11**) [32], pyripyropene A(**12**) [33], bisdethiobis-(methylthio)gliotoxin (**13**) [34], fumagillin (**14**) [35], methylemodine (**15**) [36], ergosterol (**16**) [16], orsellinic acid (**17**) [37], orcinol (**18**) [38], indolyl-3-acetic acid (**19**), indolyl-3-acetic acid methyl ester (**20**) [39], *p*-hydroxybenzoic acid (**21**), pyrrole-2-carboxylic acid (**22**) and pyrrole-3-carboxylic acid (**23**) [40] (Fig. 1). Structures of all isolated compounds were determined by 1D and 2D NMR, and mass spectrometric data and comparison with literature (see supplementary file).

2.3. Biological Activity

2.3.1. Antimicrobial activity

The antibacterial activity of the strain extract was visualized against five pathogenic bacterial strains: *Escherichia coli* DSMZ 1058, *Bacillus subtilis* DSMZ 704, *Micrococcus luteus* DMSZ 1605, *Pseudomonas agarici* DSMZ 11810, *Staphylococcus warneri* DSMZ 20036 using agar-diffusion test method on sterilized paper disk (6 mm). However, no antibacterial activity was displayed from the strain extract against any of the bacterial strains tested.

2.3.2. Cytotoxic activity study

The *in vitro* anticancer activity of selected compounds (fumitremorgine C (**6**), cyclotryprostatin B (**4**), 20-hydroxycycloprostatin B (**5**), 12,13-dihydroxy fumitremorgine C (**7**), pseurotin A (**8**), azaspirofuran A (**9**), orselinic acid (**17**), orcinol (**18**)) based on their quantities and structural classifications, against the non-small cell lung cancer (NSCLC) A549 using XTT method was investigated. According to this study, no significant cytotoxicity was remarked for orselinic acid (**17**) and orcinol (**18**) (due mostly to their very small molecular sizes and highly charged particles) and 20-Hydroxycycloprostatin B (**5**). On the other hand, cyclotryprostatin B (**4**) showed cytotoxcity against A549 cell line with IC_{50} of ~100 μM, meanwhile pseurotin A (**8**) and azaspirofuran A (**9**) showed IC_{50} in the range of 51-100 μM. In contrast, fumitremorgine C (**6**) is neurotoxic and hence it cannot be used clinically. Furthermore, the anticancer activity of benzoyltryptophane (**1**) and orcinol (**18**) against cervix carcinoma cell line (KB-3-1), revealed no cytotoxicity.

2.3.3. Molecular docking and anti-SARS-CoV-2 activity

The compounds were scanned as possible agents against SARS-CoV-2 proteins; 3C-like protease (3CLpro), papain-like protease (PLpro), and spike protein S using automated molecular docking. The inhibitory process could be achieved by blocking the replication and the transcription of the virus in the case of the two proteases or by the interference of the virus-cell recognition in the case of the spike protein [41,42].

The viral spike (S) glycoprotein interacts with the host cell *via* its RBD moiety which binds to the angiotensin-converting enzyme 2 (ACE2) receptor to invade the human cell. The spike protein which consists of two subunits, S_1 and S_2, interacts with the ACE2 receptor *via* the S_1 subunit [43-45]. This interaction may be interrupted by introducing a drug candidate which could disrupt the recognition process at the interface of the S_1/ACE2 heteroisomer [18, 46]. The recently available 3D structure of the S_1 unit during the recognition phase with the ACE2 full protein was selected for the *in*-silico study [44]. The RBD pocket that is in the region of the interfacial site between the viral and the eukaryotic protein was aimed by our structures and no favorable candidate was observed with exception of chaetominine (**2**), fumitremorgin C (**6**) and azaspirofuran A (**9**). They had an energy of interaction of -8.3, -9.0, and -8.1 Kcal/mol in their most stable poses (Figs. 2 and 3). These poses interacted with ACE2 away from the interface between the viral and the host protein, suggesting their lack of efficacy in this proposed activity. Their binding poses located inside the RBD groove had higher binding energy besides they weren't subsidized with enough hydrogen bonds. From this simulation, no candidate of the current library could be assumed as a disruptor of the viral invasion phase.

For 3CLpro, most of them were not susceptible to being active against this target except chaetominine (**2**), fumitremorgin C **6**) and azaspirofuran A (**9**). They had the energy of interaction of -9.0, -8.1 and -8.1 kcal/mol respectively. However, these stable binding modes hadn't sufficient hydrogen bonds implicated in the interaction that may disallow them from being drug candidates. Meanwhile, the second protease (PLpro) was affected by the same compounds in addition to pseurotin A (**8**). The binding energy was between -9.4 and -8.0 kcal/mol for the poses with the lowest RMSD values. Nevertheless, chaetominine (**2**) was the only compound that formed a satisfying number of hydrogen bonds with Glu167, Tyr264, and Met208 and the binding energy was -8.8 kcal/mol for the selected pose with RMSD of 5.809. The pose with lower binding energy (-9.4 kcal/mol) was

excluded since it formed no hydrogen bond with the target. On the other hand, the low values of binding energy which mean higher affinity of the previously mentioned structures may suggest an influence of hydrophobic interaction in the stabilization of the drug-protein complex. This proposition needs to be confirmed by biological analysis.

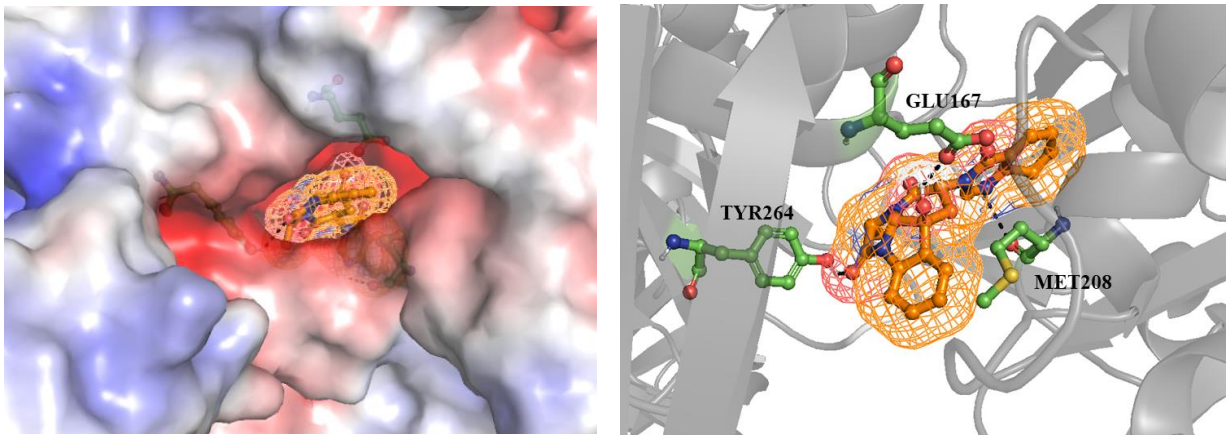

Figure 2. Chaetominine (**2**) showed as sticks and ball inside a mesh inserted deeply within the pocket of papain-like protease (PLpro) (left image), it formed three hydrogen bonds with the adjacent amino acids Glu167, Tyr264 and Met208 showed as green sticks (right image)

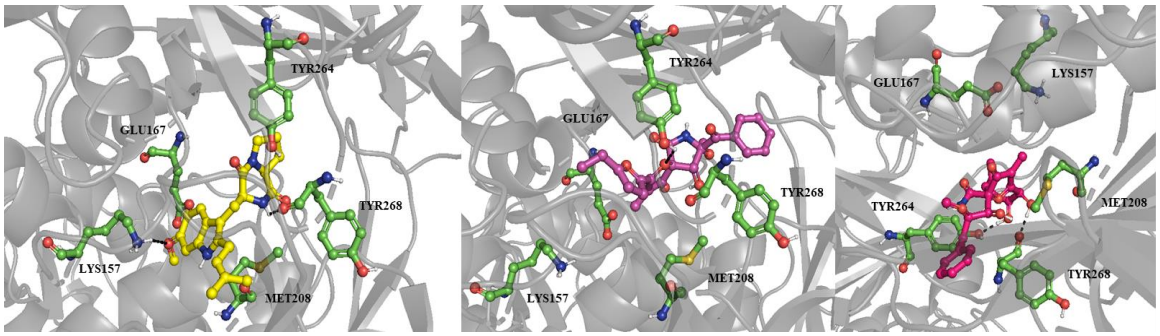

Figure 3. The poses of fumitremorgin C (**6**, yellow stick), azaspirofuran A (**9**, pink stick) and pseurotin A (**8**) inside the binding site of PLpro, hydrogen bonds were shown as black dashes.

2.3.4. Study of the anti-SARS-CoV-2 activity according to Molecular docking visualization

The *in vitro* anti-SARS-CoV-2 analysis was explored using the most promising compounds according to the molecular docking study. Fumitremorgin C (**6**) showed the highest promising antiviral activity (Fig. 4), with CC_{50} (the concentration required to cause a 50% toxicity of the normal Vero E6 cells) of 193.8 µg/ml, and IC_{50} (the concentration required to cause 50% viral inhibition) is 9.8 µg/ml, and selectivity index of SI = 20.3. On the other hand, both azaspirofuran A (**9**) and chaetominine (**2**) showed higher safety than fumitremorgin C (**6**), with CC_{50} value of 6075 and 7894 µg/ml, respectively. However, azaspirofuran A (**9**) and chaetominine (**2**) showed moderate antiviral activities compared to fumitremorgin C (**6**), and their selectivity indices were 3.2, and 6.6 respectively. The SARS-CoV-2 viral inhibitory concentration IC_{50} is 1874 µg/ml for azaspirofuran A (**9**) and 1196 µg/ml for chaetominine (**2**).

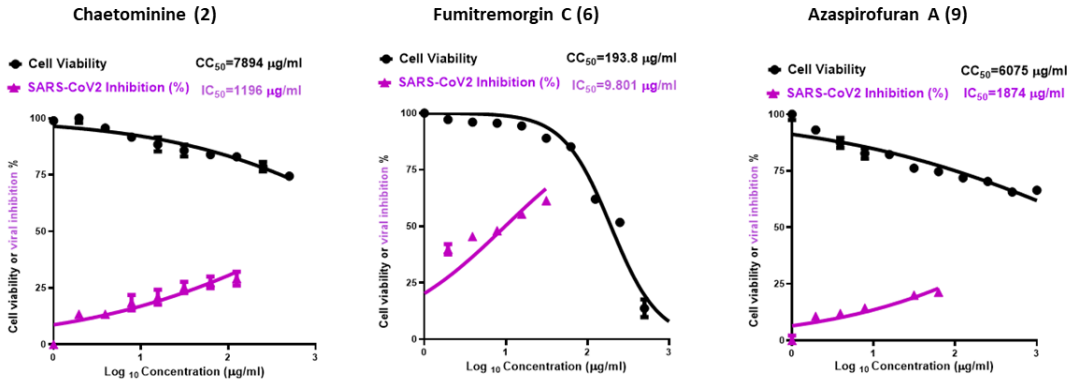

Figure 4. Graph of cytotoxicity concentration (CC_{50}) and inhibitory concentration (IC_{50})

3. Materials and Methods

3.1. General Experimental Details

Column chromatography was carried out on silica gel (0.06–0.2 mm, Merck, Darmstadt, Germany). Gel filtration was carried out on Sephadex LH-20 (GE Healthcare, Uppsala, Sweden). Preparative TLC (0.5 mm thick) and analytical TLC was performed on Merck pre-coated silica gel 60 $PF_{254+366}$ plates (Merck, Darmstadt, Germany). *R*fvalues of the bioactive compounds and visualization of their chromatograms was carried out under UV light (254 and 366 nm) and further by spraying with anisaldehyde/sulfuric acid followed by heating. High Resolution ESI-MS was done on a Micromass AC-TOF micro mass spectrometer (Micromass, Agilent Technologies 1200 series, Waldbronn, Germany). Optical rotations were measured on a P-1020 polarimeter (JASCO, Tokyo, Japan). 1D NMR and 2D (COSY, HMQC, HMBC, NOESY) NMR spectra were recorded on an Avance 500 MHz spectrometer (Bruker, Rheinstetten, Germany) at 500 MHz (^{1}H) and 125 MHz (^{13}C) at 298 K using the residual solvent peaks as a reference.

3.2. Aspergillus Terreus LGO13: Isolation, and taxonomic characterization

Details of the experimental isolation and taxonomic characterization of the producing fungus were reported previously [2, 16]. A pure colony of the strain has been cultivated on potato-dextrose agar (PDA) and kept in the fridge at 4°C. *A. terreus* strain LGO13 is deposited in Microbial Chemistry Department, National Research Centre (NRC), Egypt.

3.3. Large-scale fermentation, working up, and isolation

Under aseptic conditions, the spore suspension of *Aspergillus terreus* LGO13 (106 spore/mL) has been used to inoculate two batches of sterilized 100 × 1 L-Erlenmeyer flasks using linear shaker containing M_2 medium followed by cultivation for 14 days at 28◦C. After cultivation, the culture broth was mixed with mycelia (2 kg) and filtered using a filter press. The afforded mycelial cake was soaked in methanol, followed by filtration, concentration, and the obtained water residue was re-extracted by ethyl acetate. The supernatant was extracted with ethyl acetate. Ethyl acetate extracts of mycelia and supernatant were combined and applied to *in vacuo* concentration till dryness using a rotary evaporator affording 13.4 g yellowish-orange crude extract.

The crude extract (13.4 g) was subjected to a silica gel column chromatography (60×3 cm). A stepwise elution of the column with cyclohexane–DCM–MeOH gradient [0.5 L cyclohexane: DCM (1:1), 1L DCM, 1.5 L DCM: MeOH (99:1), 0.5L DCM: MeOH (97:3), 0.5L DCM: MeOH (95:5), 0.5L DCM: MeOH (90:10)] monitored by TLC resulted in five fractions. Fraction 1 (2.32 g) was subjected to silica gel column (60×1.5 cm) using cyclohexane-DCM gradient to afford colorless crystals of ergosterol (**16**, 220 mg).Fraction 2 (3.57 g) was further fractionated using silica gel column to afford two sub-fractions F2a and F2b. Applying of both sub-fractions individually to silica gel columns, eluted with cyclohexane-DCM-MeOH gradient, afforded helvolic acid (**11**, 5 mg), pyripyropene A (**12**, 7 mg),

bisdethiobis-(methylthio)gliotoxin (**13**, 50 mg) and indolyl-3-acetic acid methyl ester (**20**, 1 mg) from F2a while F2b delivered fumitremorgin C (**6**, 300 mg), 12,13-dihydroxy-fumitremorgin C (**7**, 4 mg), azaspirofuran A (**9**, 80 mg), fumagillin (**14**, 95 mg) and methylemodine (**15**, 1.5 mg). With similar procedure carried out for fraction 2, fraction 3 (2.68 g) was purified to give sub-fractions F3a and F3b and their subsequent purification gave cyclotryprostatin B (**4**, 1.5 mg) and pseurotin A (**9**, 68 mg) from F3a while F3b gave chaetominine (**2**, 54 mg), orsellininc acid (**17**, 30 mg), orcinol (**18**, 26 mg), indolyl-3-acetic acid (**19**, 1.6 mg), p-hydroxybenzoic acid (**21**, 2.6 mg), pyrrole-2-carboxylic acid (**22**, 1.7 mg), and pyrrole-3-carboxylic acid (**23**, 1.3 mg). Gel-fitration of fraction 4 (1.78 g) on Sephadex LH-20 (CH_2Cl_2/40% MeOH) yielded two sub-fractions F4a and F4b. Fumigaclavine C (**3**, 40 mg), 20-hydroxycyclotryprostatin B (**5**, 15 mg), and terezine D (**10**, 6.5 mg) were obtained from F4a after their application to silica gel column using DCM-MeOH gradient. A final purification of the last fraction 5 (0.63 g) using Sephadex LH-20 (DCM/40% MeOH) afforded *N*-benzoyl-tryptophane (**1**, 13 mg) as a colorless solid.

3.4. Antimicrobial Activity Assay

Antimicrobial activity testing of the microbial extract and obtained compounds were carried out against a set of microorganisms using paper-disk diffusion assay [47] with some modifications according to our previous work [48].

3.5. Cytotoxicity Assays

The XTT cell viability assay (Roche Diagnostics, Filderstadt, Germany) is a colorimetric assay that measures cellular metabolic activity. The assay is based on the mitochondrial reduction of tetrazolium salt by viable cells with active mitochondrial dehydrogenase into the orange-colored water-soluble formazan salt. Different types of cancer cells were plated in 96-well microtiter plates and treated with different concentrations of the respective compounds for 48 h before incubating with XTT labeling mixture at 37 °C [49]. The spectrophotometric absorbance was measured using a TECAN Infinite® 200 PRO microplate reader (Männedorf, Switzerland) at 450 nm with a 630 nm-reference filter. Paclitaxel (MP Biomedicals, Santa Ana, CA) served as a positive control.

3.5. Anti-coronavirus activity molecular docking

All crystallographic structures were downloaded from the protein data bank (PDB codes of 3CLpro, PLpro, and spike glycoprotein= 6LU7, 6WUU, and 6M17 respectively) [44,50,51]. The compounds were designed by ChemDraw and prepared for docking by VEGA which was used as well for the enzyme preparation (deleting water and the native ligands, etc.) [52]. The grid boxes were placed in the binding sites of the native ligands of 3CLpro and PLpro. On the other hand, the other grid box was positioned in the interfacial region between the S1 unit and ACE2 for the spike protein during the Molecular docking simulation. Docking was processed by Autodock vina, and the binding poses, and the hydrogen bond formation was detected by Pymol [53,54].

3.6. Anti-SARS-CoV-2 activity Assays

3.6.1. Cytotoxicity assay

To assess the half maximal cytotoxic concentration (CC_{50}), stock solutions of the test compounds were prepared in 10 % DMSO in deionized H_2O and diluted further to the working solutions with DMEM. The cytotoxic activity of the extracts was tested in VERO-E6 cells by using the 3-(4, 5-dimethylthiazol -2-yl)-2, 5-diphenyltetrazolium bromide (MTT) method with minor modifications. Briefly, the cells were seeded in 96 well-plates (100 µl/well at a density of 3×10^5 cells/ml) and incubated for 24 h at 37 °C in 5%CO_2. After 24 h, cells were treated with various concentrations of the tested compounds in triplicates. 24 h later, the supernatant was discarded, and cell monolayers were washed with sterile 1x phosphate buffer saline (PBS) 3 times and MTT solution (20 µl of 5 mg/ml stock solution) was added to each well and incubated at 37 °C for 4 h followed by medium aspiration. In each well, the formed formazan crystals were dissolved with 200 µl of acidified isopropanol (0.04 M HCl in absolute isopropanol = 0.073 ml HCL in 50 ml isopropanol).

Absorbance of formazan solutions was measured at λ max 540 nm with 620 nm as a reference wavelength using a multi-well plate reader. The percentage of cytotoxicity compared to the untreated cells was determined with the following equation. The plot of % cytotoxicity versus sample concentration was used to calculate the concentration which exhibited 50% cytotoxicity (CC_{50}) [55].

$$\text{Cytotoxicity \%} = \frac{(\text{Absorbance of cells without treatment- Absorbance of cells with treatment}) \times 100}{\text{Absorbance of cells without treatment}}$$

3.6.2. Inhibitory concentration 50 (IC_{50}) determination

In 96-well tissue culture plates, 2.4×10^4 Vero-E6 cells were distributed in each well and incubated overnight at a humidified 37°C incubator under 5%CO_2 condition. The cell monolayers were then washed once with 1x PBS and subjected to virus adsorption (hCoV-19/Egypt/NRC-03/2020 (Accession Number on GSAID: EPI_ISL_430820)) for 1 h at room temperature (RT). The cell monolayers were further overlaid with 100µl of DMEM containing varying concentrations of the test compounds. Following incubation at 37°C in 5% CO_2 incubator for 72 h, the cells were fixed with 100 µl of 4% paraformaldehyde for 20 min and stained with 0.1% crystal violet in distilled water for 15 min at RT. The crystal violet dye was then dissolved using 100 µl absolute methanol per well and the optical density of the color is measured at 570 nm using Anthos Zenyth 200rt plate reader (Anthos Labtec Instruments, Heerhugowaard, Netherlands). The IC_{50} of the compound is that required to reduce the virus-induced cytopathic effect (CPE) by 50%, relative to the virus control [56].

5. Conclusions

In this study, twenty-three diverse bioactive metabolites were investigated from the marine *Aspergillus terreus* LGO13 after its re-cultivation using liquid culture fermentation. Their structures were established based on HR-ESIMS 1D/2D NMR spectroscopy, and comparison with literature data. The antimicrobial, cytotoxicity, and antiviral activities of the microbial extract and the obtained compounds were investigated using a set of microorganisms, cervix carcinoma KB-3-1, non-small cell lung cancer (NSCLC) A549, and coronavirus (SARS-CoV-2), respectively. Molecular docking (MD) simulation was employed exploring the promising targets of the isolated metabolites as anti-SARS-CoV-2 agents. Particularly, chaetominine (**2**) was established as potential candidate against papain-like protease (PLpro). We accordingly assessed the antiviral efficacy of chaetominine (**2**), fumitremorgin C (**6**), and azaspirofuran A (**9**) against SARS-CoV-2 inspired by the MD results. Fumitremorgin C (**6**) showed a high selectivity index (SI = 20.3), while chaetominine (**2**) and azaspirofuran A (**9**) showed moderate selectivity index (SI = 6.6 and 3.2, respectively). These results showed a promising antiviral activity of Fumitremorgin C against SARS-CoV-2 virus, suggesting them to be further in vivo studied hopefully be served as drug candidate in the overcoming of the SARS-CoV-2.

Supplementary Materials: The following are available online at https://www.mdpi.com/article/10.3390/md19120715/s1,

Author Contributions: Conceptualization, M.S., A.H.; methodology, A.H, M.S., A.B.A, A.E., M.G.; validation, M.S., A.H., A.B.A, A.E., M.G ; formal analysis, M.S., A.H., A.B.A.; investigation, A.H, M.S., A.B.A, A.E., M.G.; resources, M.S., N.S; data curation, M.S., A.H., A.B.A, A.E., M.G. and N.S.; writing—Original draft preparation, A.H., M.S., A.B.A., A.E., M.G.; writing—Review and editing, A.H., M.S., A.B.A., A.E., M.G., N.S.; visualization, A.H., M.S., A.B.A., A.E., M.G., N.S.; supervision, M.S., N.S.; project administration, M.S. and N.S.; funding acquisition, N.S. All authors have read and agreed to the published version of the manuscript.

Funding: This research work has been financed by the German Academic Exchange Service (DAAD) with funds from the German Federal Foreign Office in the frame of the Research Training Network "Novel Cytotoxic Drugs from Extremophilic Actinomycetes" (Project ID 57166072).

Institutional Review Board Statement: Not applicable.

Data Availability Statement: Further data are available on request from the corresponding author.

Acknowledgments: The authors are thankful to the NMR and MS Departments in Bielefeld University for the spectral measurements. We thank Carmela Michalek for her assistance in biological activity testing; Marco Wißbrock and Anke Nieß for technical assistance.

Conflicts of Interest: The authors declare no conflict of interest.

References

1. Abdel-Razek, A.S.; El-Naggar M.E.; Allam A.; Morsy O.M.; Othman S.I. Microbial Natural Products in Drug Discovery. *Processes* **2020**, *8*, 470. https://doi.org/10.3390/pr8040470.
2. Abdel-Razek A.S.; Hamed, A.; Frese M.; Sewald N.; Shaaban M. Penicisteroid C: New polyoxygenated steroid produced by co-culturing of *Streptomyces piomogenus* with *Aspergillus niger*. *Steroids* **2018**, *138*, 21–25. https://doi.org/10.1016/j.steroids.2018.06.005.
3. Laatsch, H.; AntiBase, A. Data Base for Rapid Structural Determination of Microbial Natural Products, and Annual Updates; Wiley-VCH: Weinheim, Germany **2017**.
4. Jin, L.; Quan, C.; Hou, X.; Fan, S. Potential pharmacological resources: natural bioactive compounds from marine-derived fungi. *Mar. Drugs* **2016**, *14*, 76. https://doi.org/10.3390/md14040076.
5. El-Kashef, D.H.; Youssef, F.S.; Hartmann, R.; Knedel, T.-O.; Janiak, C.; Lin, W.; Reimche, I.; Teusch, N.; Liu, Z.; Proksch, P. Azaphilones from the Red Sea fungus *Aspergillus Falconensis*. *Mar. Drugs* **2020**, *18*, 204. https://doi.org/10.3390/md18040204.
6. Schueffler, A.; Anke, T. Fungal natural products in research and development. *Nat. Prod. Rep.* **2014**, *31*, 1425–1448. https://doi.org/10.1039/C4NP00060A.
7. Youssef, F.S.; Ashour, M.L.; Singab, A.N.B.; Wink, M. A comprehensive review of bioactive peptides from Marine fungi and their biological significance. *Mar. Drugs* **2019**, *17*, 559. https://doi.org/10.3390/md17100559.
8. Yoon, J.; Kikuma, T.; Maruyama, J.; Kitamoto, K. Enhanced production of bovine chymosin by autophagy deficiency in the filamentous fungus *Aspergillus oryzae*. *PloS one*. **2013**, *8*, e62512. https://doi.org/10.1371/journal.pone.0062512.
9. Singh, B.K.; Park, S.H.; Lee, H-B.; Goo, Y-A.; Kim, H.S.; Cho, S.H.; Lee, J.H.; Ahn, G.W.; Kim, J.P.; Kang, S.M.; Kim. E-K. Kojic Acid Peptide: A New Compound with Anti-Tyrosinase Potential. *Ann. Dermatol*. **2016**, 28:555–561. https://doi.org/10.5021/ad.2016.28.5.555.
10. Then Bergh, K.; Brakhage A.A. Regulation of the Aspergillus nidulans penicillin biosynthesis gene acvA (pcbAB) by amino acids: implication for involvement of transcription factor PACC. *Appl. Environ. Microbiol*. **1998**, *64*, 843–849. https://doi.org/10.1128/AEM.64.3.843-849.1998
11. Fu, Y.; Wu, P.; Xue, J.; Wei, X.; Li, H. Versicorin, a new lovastatin analogue from the fungus Aspergillus versicolor SC0156. *Nat. Prod. Res*. **2015**, *29*, 1363–1368. https://doi.org/10.1080/14786419.2015.1026342.
12. Kang, H.K.; Lee, H.H.; Seo, C.H.; Park, Y. Antimicrobial and immunomodulatory properties and applications of marine-derived proteins and peptides. *Mar. Drugs* **2019**, *17*, 350. https://doi.org/10.3390/md17060350.
13. Zhang, X.; Li, Z.; Gao, J. Chemistry and biology of secondary metabolites from Aspergillus genus. Nat. Prod. J. **2018**, 8, 275–304. doi: 10.2174/2210315508666180501154759.
14. He, F.; Bao, J.; Zhang, X.-Y.; Tu, Z.-C.; Shi, Y.-M.; Qi, S.-H. Asperterrestide A, a cytotoxic cyclic tetrapeptide from the marine derived fungus *Aspergillus terreus* SCSGAF0162. *J. Nat. Prod*. **2013**, *76*, 1182–1186. https://doi.org/10.1021/np300897v.
15. Youssef, F.S.; Alshammari E.; Ashour, M.L. Bioactive Alkaloids from Genus Aspergillus: Mechanistic Interpretation of Their Antimicrobial and Potential SARS-CoV-2 Inhibitory Activity Using Molecular Modelling. *Int. J. Mol. Sci*. **2021**, *22*, 1866. https://doi.org/10.3390/ijms22041866.
16. Hamed, A.; Abdel-Razek, A.S.; Omran, D.A.; El-Metwally, M.M.; El-Hosari, D.G.; Frese, M.; Soliman, H.S.M.; Sewald, N.; Shaaban M. Terretonin O: a New Meroterpenoid from *Aspergillus terreus* Strains TM8 and LGO13. *Nat. Prod. Res*. **2020**, *34*, 965-974. https://doi.org/10.1080/14786419.2018.1544977.
17. Shaaban, M.; El-Metwally, M.M.; Abdel-Razek, A.A.; Laatsch, H. Terretonin M: A new meroterpenoid from the thermophilic *Aspergillus terreus* TM8 and revision of the absolute configuration of penisimplicins. *Nat. Prod. Res.* **2018**, *32*, 2437-2446. https://doi.org/10.1080/14786419.2017.1419230.
18. Murugan, N.A.; Kumar, S.; Jeyakanthan, J.; Srivastava, V. Searching for Target-Specific and Multi-Targeting Organics for Covid-19 in the Drugbank Database with a Double Scoring Approach. *Sci. Rep.* **2020**, *10*, 19125. https://doi.org/10.1038/s41598-020-75762-7.
19. Weiss, S.R.; Leibowitz J.L. Coronavirus pathogenesis. *Adv. Virus Res*. **2011**, *81*, 85-164. https://doi.org/10.1016/B978-0-12-385885-6.00009-2.
20. Elfiky, A.A. Ribavirin, Remdesivir, Sofosbuvir, Galidesivir, and Tenofovir against SARS-CoV-2 RNA dependent RNA polymerase (RdRp): A molecular docking study. *Life Sci*. **2020**, *253*, 117592. https://doi.org/10.1016/j.lfs.2020.117592.
21. Sarhan, A.A.; Ashour N.A.; Al-Karmalawy A.A. The journey of antimalarial drugs against SARS-CoV-2: Review article. *Inform. Med. Unlocked* **2021**, *24*, 100604. https://doi.org/10.1016/j.imu.2021.100604.

22. Kutkat, O.; Moatasim Y.; Al-Karmalawy, A.A.; Abulkhair, H.S.; Gomaa M.R.; El-Taweel, A.N.; Abo Shama, N.M.; GabAllah, M.; Mahmoud, D.B.; Kayali, G.; Ali, M.A.; Kandeil A.; Mostafa A. Robust antiviral activity of commonly prescribed antidepressants against emerging coronaviruses: *in vitro* and *in silico* drug repurposing studies. *Sci. Rep.* **2022**, *12*, 12920. https://doi.org/10.1038/s41598-022-17082-6.
23. Shaaban, M.; Abdel-Razek, A.S.; Previtali, V.; Clausen, M.H.; Gotfredsen, C.H.; Laatsch, H.; Ding L. Sulochrins and alkaloids from a fennel endophyte *Aspergillus* sp. FVL2. *Nat. Prod. Res.* **2023**, *37*, 1310-1320. https://doi.org/10.1080/14786419.2021.2005054.
24. Jiao, R.H.; Xu, S.; Liu, J.Y.; Ge, H.M.; Ding, H.; Xu, C.; Zhu, H.L.; Tan, R.X. Chaetominine, a Cytotoxic Alkaloid Produced by Endophytic Chaetomium sp. IFB-E015. *Org. Lett.* **2006**, *8*, 5709–5712. https://doi.org/10.1021/ol062257t.
25. He, F.; Sun, Y.L.; Liu, K.S.; Zhang X.Y.; Qian, P.Y.; Wang, Y.F.; Qi S.H. Indole alkaloids from marine-derived fungus *Aspergillussydowii* SCSIO 00305. *J. Antibiot.* **2012**, *65*, 109–111. https://doi.org/10.1038/ja.2011.117.
26. Zhang, Y-H.; Geng, C.; Zhang, X-W.; Zhu, H-J.; Shao, C-L.; Cao, F.; Wang, C-Y. Discovery of Bioactive Indole-Diketopiperazines from the Marine-Derived Fungus *Penicillium brasilianum* Aided by Genomic Information. *Mar. Drugs*. **2019**, **17**, 514. https://doi.org/10.3390/md17090514.
27. Rabindran S.K.; Ross, D.D.; Doyle, L.A.; Yang, W.; Greenberger, L.M. Fumitremorgin C reverses multidrug resistance in cells transfected with the breast cancer resistance protein. *Cancer Res.* **2000**, *60*, 47-50.
28. Abraham, W-R.; Arfmann, H-A. 12,13-Dihydroxy-fumitremorgin C from *Aspergillus fumigatus*. *Phytochemistry* **1990**, *29*, 1025-1026. https://doi.org/10.1016/0031-9422(90)80080-Z.
29. Ishikawa, M.; Ninomiya, T.; Akabane, H.; Kushida, N.; Tsujiuchi, G.; Ohyama, M.; Gomi, S.; Keiko Shito, K.; Murata, T. Pseurotin A and its analogues as inhibitors of immunoglobuline E production. *Bioorg. Med. Chem. Lett.* **2009**, *19*, 1457–1460. https://doi.org/10.1016/j.bmcl.2009.01.029.
30. Copmans, D.; Rateb, M.; Tabudravu, J.N.; Pérez-Bonilla, M.; Dirkx, N.; Vallorani, R.; Diaz, C.; del Palacio, J.P.; Smith, A.J.; Ebel, R.; Reyes, F.; Jaspars, M.; de Witte, P. A. M. Zebrafish-Based Discovery of Antiseizure Compounds from the Red Sea: Pseurotin A2 and Azaspirofuran A. *ACS Chem. Neurosci.* **2018**, *9*, 1652–1662. https://doi.org/10.1021/acschemneuro.8b00060.
31. Wang, Y.; Gloer, J.B.; Scott, J.A.; Malloch, D. Terezines A-D: new amino acid-derived bioactive metabolites from the coprophilous fungus *Sporormiella teretispora*. *J. Nat. Prod*. **1995**, *58*, 93-99. https://doi.org/10.1021/np50115a011.
32. Ratnaweera, P.B.; Williams, D.E.; de Silva, E.D.; Wijesundera, R.L.C.; Dalisay, D.S.; Andersen, R.J. Helvolic acid, an antibacterial nortriterpenoid from a fungal endophyte, *Xylaria* sp. of orchid *Anoectochilussetaceus* endemic to Sri Lanka. *Mycology* **2014**, *5*, 23-28. https://doi.org/10.1080/21501203.2014.892905.
33. Odani, A.; Ishihara, K.; Ohtawa, M.; Tomoda, H.; Omura, S.; Nagamitsu, T. Total synthesis of pyripyropene A. *Tetrahedron* **2011**, *67*, 8195–8203. https://doi.org/10.1016/j.tet.2011.06.084.
34. Lee H.J.; Lee J.H.; Hwang B.Y.; Kim H.S.; Lee J.J. Anti-angiogenic activities of gliotoxin and its methylthio-derivative, fungal metabolites. *Arch. Pharm. Res.* **2001**, *24*, 397-401.
35. Guruceaga, X.; Perez-Cuesta, U.; de Cerio, A.A-D.; Gonzalez O.; Alonso R.M.; Hernando F.L.; Ramirez-Garcia A.; Rementeria A. Fumagillin, a Mycotoxin of *Aspergillus fumigatus*: Biosynthesis, Biological Activities, Detection, and Applications. *Toxins* **2020**, *12*, 7. https://doi.org/10.3390/toxins12010007.
36. Yang, Y.; Yan, Y.-M.; Wei, W.; Luo, J.; Zhang, L.-S.; Zhou, X.-J.; Wang, P.-C.; Yang, Y.-X.; Cheng, Y.-X. (2013). Anthraquinone derivatives from Rumex plants and endophytic Aspergillus fumigatus and their effects on diabetic nephropathy. *Bioorg. Med. Chem. Lett.* **2013**, *23*, 3905–3909. https://doi.org/10.1016/j.bmcl.2013.04.059.
37. Braesel, J.; Fricke, J.; Schwenk, D.; Hoffmeister, D. Biochemical and genetic basis of orsellinic acid biosynthesis and prenylation in a stereaceous basidiomycete. *Fungal Genet. Biol.* **2017**, *98*, 12–19. https://doi.org/10.1016/j.fgb.2016.11.007.
38. Eliwa, E.M.; Abdel-Razek, A.S.; Frese, M.; Halawa, A.H.; El-Agrody, A.M.; Bedair, A.H.; Sewald, N.; Shaaban, M. New naturally occurring phenolic derivatives from marine Nocardiopsis sp. AS23C: Structural elucidation and *in silico* computational studies. *Vietnam J. Chem*. **2019**, *57*, 164-174. https://doi.org/10.1002/vjch.201900010.
39. Hamed, A.; Abdel-Razek, A.S.; Frese, M.; Wibberg, D.; El-Haddad, A.F.; Ibrahim, T.M.A.; Kalinowski J.; Sewald N.; Shaaban, M. N-Acetylborrelidin B: a new bioactive metabolite from *Streptomyces mutabilis* sp. MII. *Z. Naturforsch. C* **2018**, *73*, 49–57. https://doi.org/10.1515/znc-2017-0140.
40. Shaaban, M. Bioactive Secondary Metabolites from Marine and Terrestrial Bacteria: Isoquinolinequinones, Bacterial Compounds with a Novel Pharmacophor. Ph.D. Thesis, Georg-August University, Göttingen, Germany, **2004**.
41. Skoreński, M.; Sieńczyk, M. Viral Proteases as Targets for Drug Design. *Curr. Pharm. Des.* **2013**, *19*, 1126–1153. doi:10.2174/1381612811319060013.
42. Li, F. Receptor Recognition Mechanisms of Coronaviruses: A Decade of Structural Studies. *J. Virol.* **2015**, *89*, 1954–1964. doi:10.1128/JVI.02615-14.
43. Huang, Y.; Yang, C.; Xu, X.; Xu, W.; Liu, S. Structural and Functional Properties of SARS-CoV-2 Spike Protein: Potential Antivirus Drug Development for COVID-19. *Acta Pharmacol. Sin.* **2020**, *41*, 1141–1149. doi:10.1038/s41401-020-0485-4.
44. Yan, R.; Zhang, Y.; Li, Y.; Xia, L.; Guo, Y.; Zhou, Q. Structural Basis for the Recognition of SARS-CoV-2 by Full-Length Human ACE2. *Science* **2020**, *367*, 1444–1448. doi:10.1126/science.abb2762.
45. Walls, A.C.; Park, Y.-J.; Tortorici, M.A.; Wall, A.; McGuire, A.T.; Veesler, D. Structure, Function, and Antigenicity of the SARS-CoV-2 Spike Glycoprotein. *Cell* **2020**, *181*, 281-292.e6. doi:10.1016/j.cell.2020.02.058.
46. Deganutti, G.; Prischi, F.; Reynolds, C.A. Supervised Molecular Dynamics for Exploring the Druggability of the SARS-CoV-2 Spike Protein. *J. Comput. Aided Mol. Des.* **2021**, *35*, 195–207. doi:10.1007/s10822-020-00356-4.

47. Bauer, A. W.; Kirby, W. M.; Sherris, J. C.; Truck, M. Antibiotic susceptibility testing by a standardized single disk method. *Am. J. Clin.Pathol.* **1966**, *45*, 493-496. https://doi.org/10.1093/ajcp/45.4_ts.493.
48. Hamed, A.; Abdel-Razek, A. S.; Frese, M.; Wibberg, D.; El-Haddad, A. F.; Ibrahim, T. M. A.; Kalinowski, J.; Sewald, N.; Shaaban, M. New oxaphenalene derivative from marine-derived *Streptomyces griseorubens* sp. ASMR4. *Z. Naturforsch. B* **2017**, *72*, 53-62. https://doi.org/10.1515/znb-2016-0145
49. Hamed, A.; Frese, M.; Elgaafary, M.; Syrovets, T.; Sewald, N.; Simmet, T.; Shaaban, M. Synthesis of novel feruloyl dipeptides with proapoptotic potential against different cancer cell lines. *Bioorg. Chem.* **2020**, *97*, 103678-103686. doi: 10.1016/j.bioorg.2020.103678.
50. Jin, Z.; Du, X.; Xu, Y.; Deng, Y.; Liu, M.; Zhao, Y.; Zhang, B.; Li, X.; Zhang, L.; Peng, C.; Duan, Y.; Yu, J.; Wang, L.; Yang, K.; Liu, F.; Jiang, R.; Yang, X.; You, T.; Liu, X.; Yang, X.; Bai, F.; Liu, H.; Liu, X.; Guddat, L.W.; Xu, W.; Xiao, G.; Qin, C.; Shi, Z.; Jiang, H.; Rao, Z.; Yang H. Structure of Mpro from SARS-CoV-2 and Discovery of Its Inhibitors. *Nature* **2020**, *582*, 289–293. doi:10.1038/s41586-020-2223-y.
51. Rut, W.; Lv, Z.; Zmudzinski, M.; Patchett, S.; Nayak, D.; Snipas, S.J.; El Oualid, F.; Huang, T.T.; Bekes, M.; Drag, M.; Olsen S.K. Activity Profiling and Crystal Structures of Inhibitor-Bound SARS-CoV-2 Papain-like Protease: A Framework for Anti-COVID-19 Drug Design. *Sci. Adv.* **2020**, *6*, eabd4596. doi:10.1126/sciadv.abd4596.
52. Pedretti, A.; Villa, L.; Vistoli, G. VEGA - An Open Platform to Develop Chemo-Bio-Informatics Applications, Using Plug-in Architecture and Script Programming. *J. Comput. Aided Mol. Des.* **2004**, *18*, 167–173. doi:10.1023/B:JCAM.0000035186.90683.f2.
53. Trott, O.; Olson, A.J. AutoDock Vina: Improving the Speed and Accuracy of Docking with a New Scoring Function, Efficient Optimization, and Multithreading. *J. Comput. Chem.* **2010**, *31*, 455–461. doi:10.1002/jcc.21334.
54. Schrodinger The PyMOL Molecular Graphics System, Version 1.8 2015.
55. Plumb, J. A. Cell sensitivity assays: the MTT assay. *Methods Mol. Med.* **2004**, *88*, 165-169. https://doi.org/10.1385/1-59259-687-8:25.
56. Feoktistova, M.; Geserick, P.; Leverkus, M. Crystal Violet Assay for Determining Viability of Cultured Cells. *Cold Spring Harb. Protoc*. **2016**, *4*, pdb prot087379. doi:10.1101/pdb.prot087379.